Cell Communication and Signaling

RESEARCH

Open Access

Senescent cells promote breast cancer cells motility by secreting GM-CSF and bFGF that activate the JNK signaling pathway

Nan Wang[1,2,3†], Yan Fang[2,7†], Yigong Hou[2,3†], Dongmei Cheng[3], Emily V. Dressler[4], Hao Wang[3,5], Juan Wang[3,8], Guanwen Wang[3,9], Yilei Li[6], Hong Liu[1], Rong Xiang[2], Shuang Yang[2*] and Peiqing Sun[3*]

Abstract

Background Cellular senescence can be induced in mammalian tissues by multiple stimuli, including aging, oncogene activation and loss of tumor suppressor genes, and various types of stresses. While senescence is a tumor suppressing mechanism when induced within premalignant or malignant tumor cells, senescent cells can promote cancer development through increased secretion of growth factors, cytokines, chemokines, extracellular matrix, and degradative enzymes, collectively known as senescence-associated secretory phenotype (SASP). Previous studies indicated that senescent cells, through SASP factors, stimulate tumor cell invasion that is a critical step in cancer cell metastasis.

Methods In the current study, we investigated the effect of senescent cells on the motility of breast cancer cells, which is another key step in cancer cell metastasis. We analyzed the motility of breast cancer cells co-cultured with senescent cells in vitro and metastasis of the breast cancer cells co-injected with senescent cells in orthotopic xenograft models. We also delineated the signaling pathway mediating the effect of senescent cells on cancer cell motility.

Results Our results indicate that senescent cells stimulated the migration of breast cancer cells through secretion of GM-CSF and bFGF, which in turn induced activation of the JNK pathway in cancer cells. More importantly, senescent cells promoted breast cancer metastasis, with a minimum effect on the primary tumor growth, in orthotopic xenograft mouse models.

Conclusions These results have revealed an additional mechanism by which senescent cells promote tumor cell metastasis and tumor progression, and will potentially lead to identification of novel targets for cancer therapies that suppress metastasis, the major cause of cancer mortality.

Keywords Breast cancer, Metastasis, Senescence, Migration, GM-CSF, bFGF, JNK

†Nan Wang, Yan Fang and Yigong Hou contributed equally to this work.

*Correspondence:
Shuang Yang
yangshuang@nankai.edu.cn
Peiqing Sun
psun@wakehealth.edu

Full list of author information is available at the end of the article

Background

Breast cancer is the leading cause of cancer mortality in women in the world [1]. Since the major cause of breast cancer mortality is distant metastasis, it is important to delineate the mechanisms that contribute to the migration and metastasis of breast cancer cells.

Senescence is a stable form of proliferative arrest in primary normal cells, resulting from exhaustion of replicative potential (replicative senescence) or exposure to stresses such as oncogene activation (oncogene-induced senescence), and is identified by a senescence biomarker, Senescence-Associated β-galactosidase (SA-β-Gal) [2]. Senescence is accompanied by increased secretion of growth factors, cytokines, chemokines, extracellular matrix, and degradative enzymes, collectively known as senescence-associated secretory phenotype (SASP) [2–4], which can change tissue microenvironments and affect nearby cells [5]. While the cell autonomous effect of senescence is to suppress cancer development by preventing the proliferation and growth of premalignant cells, senescent cells, through SASP, can damage the surrounding tissues, stimulate the proliferation of neighboring cancerous cells, promote tumor angiogenesis, and induce chronic inflammation, thus accelerating tumor progression and age-related diseases [6, 7].

Multiple studies have demonstrated that senescent stromal cells, such as senescent fibroblasts, create a tumor-promoting microenvironment through secretion of SASP factors [8]. For example, co-culture with senescent dermal fibroblasts promoted proliferation of premalignant melanoma cells and enhanced the invasion of advanced malignant melanoma cells [9]. Senescence within the stroma, especially the senescent fibroblasts, triggered tumor development [10]. The conditioned medium from senescent fibroblasts stimulated invasion of human umbilical vein endothelial cells into the basement membrane, which is a hallmark of tumor angiogenesis [2]. In a skin carcinogenic model, senescent fibroblasts promoted early skin carcinogenesis via a paracrine MMP-PAR-1 axis [11]. Furthermore, it was demonstrated that cellular senescence could promote cancer development in aged organisms [5].

These previous studies indicate that senescent cells, through SASP factors, promote tumor progression by stimulating tumor cell proliferation, and tumor cell invasion that a critical step in cancer cell metastasis. In this study, we examined the effect of senescent cells on the motility of breast cancer cells, which is another key aspect of cancer cell metastasis. Our results demonstrate that senescent fibroblasts stimulate the migration of breast cancer cells through secretion of GM-CSF and bFGF, which induce the activation of the JNK pathway in the cancer cells. These results have revealed an additional mechanism by which senescent cells promote tumor cell metastasis and tumor progression, and will potentially lead to identification of novel targets for cancer therapies that suppress metastasis, the major cause of cancer mortality.

Methods

Cell culture

MDA-MB-231 and MDA-MB-468 cell lines were maintained in DMEM (Corning, 10-017-CM) supplemented with 10% fetal calf serum (Gibco), 1% antibiotics (Gibco), 1% non-essential amino acids (NEAA) (Gibco), and 1% sodium pyruvate (Gibco). MCF-7 cell lines were maintained in GlutaMAX™ DMEM Dulbecco's Modified Eagle Medium (Gibco, 10569010) supplemented with 10% fetal calf serum (Gibco), and 1% antibiotics (Gibco). BJ human fibroblasts were cultured in MEM (Corning, 10-010-CV) supplemented with 10% fetal calf serum, 1% antibiotics, and 1% NEAA. If necessary, recombinant human bFGF (Gibco, PHG0026) and human GM-CSF (Peprotech, 300-03) were added to the medium of BJ cells at the final concentration of 10 ng/mL and 20 ng/mL, respectively. Neutralizing antibodies against bFGF (Cell Signaling, 98658) and GM-CSF (Cell Signaling, 56712) were added to the medium of BJ cells at the final concentration of 1 ng/mL and 5 ng/mL, respectively.

Plasmids and lentivirus-based gene transduction

Oligos encoding shRNAs for bFGF, GM-CSF, JNK1 and JNK2 were designed, synthesized, and inserted into pLV-H1-EF1α-puro vector (Biosettia) according to manufacturer's protocol. Primer and oligo sequences are listed in Supplementary data (Table S1).

Recombinant lentiviruses and retroviruses were packaged and transduced into cells as described previously [12]. Transduced cells were selected with 1 μg/ml of puromycin or 10 μg/ml blasticidin when necessary.

Protein extraction and Western blotting analysis

Protein extraction and Western blotting analysis were performed as described previously [12]. Cell lysates were prepared by incubation with 1X RIPA buffer (phosphate-buffered saline containing 1% Triton X-100, 0.5% deoxycholate, 0.1% SDS, 1 mM Na_3VO_4) with Complete Protease Inhibitor Cocktails (Roche) for 30 min on ice, followed by clearance by centrifugation at 4 °C at 15,000 g for 15 min. Protein concentrations were determined by the BCA assay. 10–50 μg of lysates were separated on 8-12% Tris-acrylamide gels and transferred to PVDF membranes. The membranes were blocked by 5% milk in 0.1% TBST for 1 h at room temperature, and incubated with primary antibodies overnight at 4 °C and with secondary antibodies (goat anti-mouse, 1:10000; goat anti-rabbit, 1:5000–7000, Cell Signaling) for 1 h at room temperature. The following primary antibodies and

concentration were used: β-actin (Santa Cruz, sc-47778 1:10000), JNK1 (Abcam, ab199380 1:1000), JNK2 (Cell Signaling, 9258 S 1:500), E-cadherin (BD Biosciences, 610181 1:1000), Vimentin (Cell Signaling, 5741 S 1:1000), p-AKT(Ser473) (Cell Signaling, 9271 S 1:1000), p-JNK (Thr183/Tyr185) (Cell Signaling, 9251 S 1:1000), JNK (Cell Signaling, 9252 1:1000), bFGF (Cell Signaling, 98658 S 1:1000), GM-CSF (Abcam, ab300495 1:1000), p-Stat3 (Ser727) (Santa Cruz, sc-8001-R, 1:1000), p-Stat3 (Tyr705) (B7, Santa Cruz, sc-8059, 1:1000), p-ERK1/2 (Thr202/Tyr204) (BIOSS, bs-3016R, 1:1000), ERK1/2 (C9, Santa Cruz, sc-514302, 1:1000).

RNA isolation, reverse transcription and qRT-PCR analysis

RNA isolation, reverse transcription and quantitative real-time PCR (qRT-PCR) analysis were performed as described previously [12]. For RNA isolation, total RNA was extracted from the cell lines using TRIzol reagent (Invitrogen, #15596-018), following the manufacturer's instructions. RNA concentration and purity were determined by measuring the absorbance at 260 nm and 280 nm using a NanoDrop spectrophotometer. Only RNA samples with a 260/280 nm absorbance ratio greater than 1.8 were considered as sufficiently pure and used for further analysis. RNA integrity and quality were confirmed by agarose gel electrophoresis.

Reverse transcription was performed using 1 μg of total RNA, employing MMLV reverse transcriptase (Promega, Madison, MI, USA) and oligo (dT) and random primers. A no-reverse transcriptase control was included in all experiments to ensure that no genomic DNA contamination was present. The synthesized complementary DNA (cDNA) was used for qRT-PCR. Primers used for PCR were designed using Primer3 software. The specificity of each primer pair was confirmed through in silico specificity screening using BLAST, to ensure that they do not amplify pseudogenes, retrosequences, or other homologous sequences. The location of each primer with respect to exons and introns was considered to avoid amplification of genomic DNA. For optimal qPCR performance, amplicon lengths were kept between 70–200 bp to ensure efficient amplification. The amplicon length for bFGF, GM-CSF, CXCL1 and GAPDH was 170 bp, 187 bp, 119 bp and 131 bp, respectively. Primers used for PCR amplification are the following. bFGF: forward 5'-AGT GTGTGCTAACCGTTACCT-3' (nucleotide 721–741, NM_002006.6), reverse 5'-ACTGCCCAGTTCGTTT CAGTG-3' (nucleotide 890−870, NM_002006.6); GM-CSF: forward 5'-TCCTGAACCTGAGTAGAGACA C-3' (nucleotide 160–181, NM_000758.4), reverse 5'-T GCTGCTTGTAGTGGCTGG-3' (nucleotide 346−328, NM_000758.4); CXCL1: forward 5'-AGCTTGCCTCAA TCCTGCATCC-3' (nucleotide 327–348, NM_001511.4), reverse 5'- TCCTTCAGGAACAGCCACCAGT-3' (nucleotide 445−424, NM_001511.4); GAPDH: forward 5'- GTCTCCTCTGACTTCAACAGCG-3' (nucleotide 920–941, NM_002046.7), reverse 5'- ACCACCC TGTTGCTGTAGCCAA-3' (nucleotide 1050−1029, NM_002046.7). qRT-PCR was conducted using PerfeCTa SYBR Green FastMix (Quantabio, USA) on an Opticon real-time PCR system (Bio-Rad, Hercules, CA, USA). For each reaction, the total volume was 20 μl, containing 10 μl of 2× PerfeCTa SYBR Green FastMix, 1 μl of each of forward and reverse primer (final concentration: 0.5 μM), and 5 μl of diluted cDNA. Each sample was run in triplicate, with three independent biological replicates. The qPCR cycling started with an initial denaturation step at 95 °C for 2 min, followed by 40 cycles of denaturation at 95 °C for 10 s, annealing and extension at 60 °C for 30 s. A melting curve analysis was performed at the end of each run to confirm the specificity of the amplification products. Primer amplification efficiencies were calculated by generating standard curves from serial dilutions of cDNA. All primers had efficiencies between 90% and 110%, and the correlation coefficient (R^2) values were ≥0.98. GAPDH was used as the reference gene for normalization, and relative gene expression levels were determined using the $2^{-\Delta\Delta Ct}$ method. All qRT-PCR data were analyzed using Bio-Rad CFX Manager software. Statistical analysis was performed using unpaired 2-sample t-tests with data from triplicates, and the results were confirmed in three independent biological repeats.

ELISA

The ELISA assays were performed with the R&D Quantikine ELISA Kit, following manufacturer's protocol, using antibodies against bFGF (Abcam, ab10420), GM-CSF (Abcam, ab9667) and CXCL1 (R&D, DGR00B).

Transwell migration assays

Cell migration assays were performed in 24-well transwell plates with 8-μm Polyethylene Terephthalate inserts (Millipore) separating lower and upper chambers, as previously described [13]. Breast cancer cells were plated in the upper chamber at 5×10^4 cells/well in serum-free medium. The lower chamber contained young or senescent BJ cells, conditioned medium from these cells, 10 ng/ml of bFGF (Gibco, PHG0026) or 20 ng/ml of GM-CSF (Peprotech, 300-03) or both, or their controls. Cells were allowed to migrate for 12–20 h. Non-migrant cells on the upper side of the filters were detached using a cotton swab. Filters were stained with 0.1% crystal violet for 1 h and photographed under microscope (KEYENCE BZ-X810). Each experiment was performed in triplicates. For each sample within the triplicates, the number of migrated cells were counted in at least 5 randomly chosen 20X fields, and the number of migrated cells per field was calculated by dividing the total number of cells by

the number of counted fields for this sample. The average number of migrated cells per field was calculated among the triplicates for the experimental group and the control groups, and compared by unpaired, 2-sample t tests between 2 groups or by One-way ANOVA for multiple comparisons using Tukey's multiple comparison correction adjustment.

Wound healing assays

MDA-MB-231, MDA-MB-468 and MCF-7 breast cancer cells were plated into 6-well plates and grown until they were confluent. The medium was replaced with conditional medium from young or senescent BJ cells containing 1% FBS or non-conditional medium containing 1% FBS. A scratch wound was made in the center of each well. Photos were taken 0, 24 (MDA-MB-231 and MDA-MB-468) or 48 (MCF-7) hours after the wound was made. The distance between the wound edges was calculated with ImageJ.

Immunofluorescence staining assays

The assays were performed in triplicates. Cells were seeded at 5×10^4/well in a 24-well plate, fixed with 4% PFA (pH7.4) for 10 min at room temperature, permeabilized in 0.1% TritonX-100, and then blocked by 3% BSA in PBS for 1 h at room temperature. The cells were incubated with the primary antibody (anti-E-cadherin, BD 610181, 1:200 dilution) overnight at 4 °C in 3% BSA in PBS, washed with PBS, and incubated with the secondary antibody (anti-mouse 488, Cell Signaling, 1:800 dilution) in 3% BSA in PBS for 1 h at room temperature. Cover slips were mounted with mounting media containing DAPI (Vector Laboratories H1200). The images were photographed under microscope (KEYENCE BZ-X810) with BZ-X viewer software. Images were quantified with the ImageJ software. The fluorescence intensity of E-cadherin was quantified in six randomly chosen 40X microscopic fields, with approximately 50–100 cells per field, for each of the triplicates.

Analysis of metastasis in orthotopic xenograft models of breast cancer

Animal protocols were approved by the Wake Forest University School of Medicine Animal Care and Use Committee, and were in accordance with the National Institutes of Health Guide for the Care and Use of Laboratory Animals. 5×10^5 of MDA-MB-231 and 5×10^5 of senescent (PD59) or young (PD22) BJ cells were co-injected into the fourth mammary fat pad of 6- to 8-week-old female nude mice in a 1:1 (vol: vol) suspension of Matrigel (BD Biosciences). Primary tumors were measured for length (a) and width (b), and the volume (V) was calculated according to the following formula: $V=ab^2\times0.52$. Tumors and lungs were harvested at the end of the experiment. Lungs were inflated and fixed by 4% paraformaldehyde, embedded with paraffin, and stained with hematoxylin and eosin. For each mouse, all 5 lung lobes were paraffin-embedded and included in the same section. The number of metastatic foci were counted in 5 randomly chosen 2X fields in each section representing each mouse, and the number of metastatic foci per field was calculated by dividing the total number of foci by 5 for this mouse. The average number of metastatic foci per field among the 6 mice in each group was calculated and compared between the senescent cell-coinjection group and the young cell-coinjection group by unpaired, 2-sample t tests.

Statistical analyses

All experiments were performed in triplicates with average values from the triplicate presented in figures. Statistical analyses were performed with Prism and SPSS software. Unpaired, 2-sample Student's t tests were performed to compare the statistical differences in an outcome between 2 groups of samples. One-way ANOVA was performed for multiple comparisons using Tukey's multiple comparison correction adjustment when more than 2 groups were considered. A p value of <0.05 was considered significant. ns indicates $p>0.05$, not significant; * indicates $p<0.05$; ** indicates $p<0.01$; and *** indicates $p<0.001$. We assessed the normality of the data distribution using Prism and the Shapiro-Wilk test, prior to performing parametric analyses (2-sample t-tests and One-way ANOVA). A p-value greater than 0.05 was considered indicative of a distribution that does not significantly deviate from normality, allowing for the use of parametric statistical tests.

Results

Senescent fibroblast-secreted factors increase the motility of breast cancer cells

To test whether senescent cells could affect the ability of breast cancer cells to migrate and metastasize, we established the senescent fibroblast model by continuously passaging the BJ fibroblasts until they reached senescence. At approximately population doubling (PD) 60 (PD56, 59, 61, 62, and 68) a substantial portion of the BJ cells displayed an enlarged and flatten morphology and were positive for the senescence associated β-galactosidase (SA-β-gal) marker, as compared to young cells at approximately PD30 (PD22, 26, 29, 31, 32, and 34), indicating the senescence state of the cells after a long period of passaging (Fig. S1). We then co-cultured the breast cancer cells with young or senescent BJ cells in different compartments of the transwells, with the breast cancer cells in the upper chamber and BJ cells in the lower chamber, and measured the migration of breast cancer cells (Fig. 1A). In 3 breast cancer cell lines

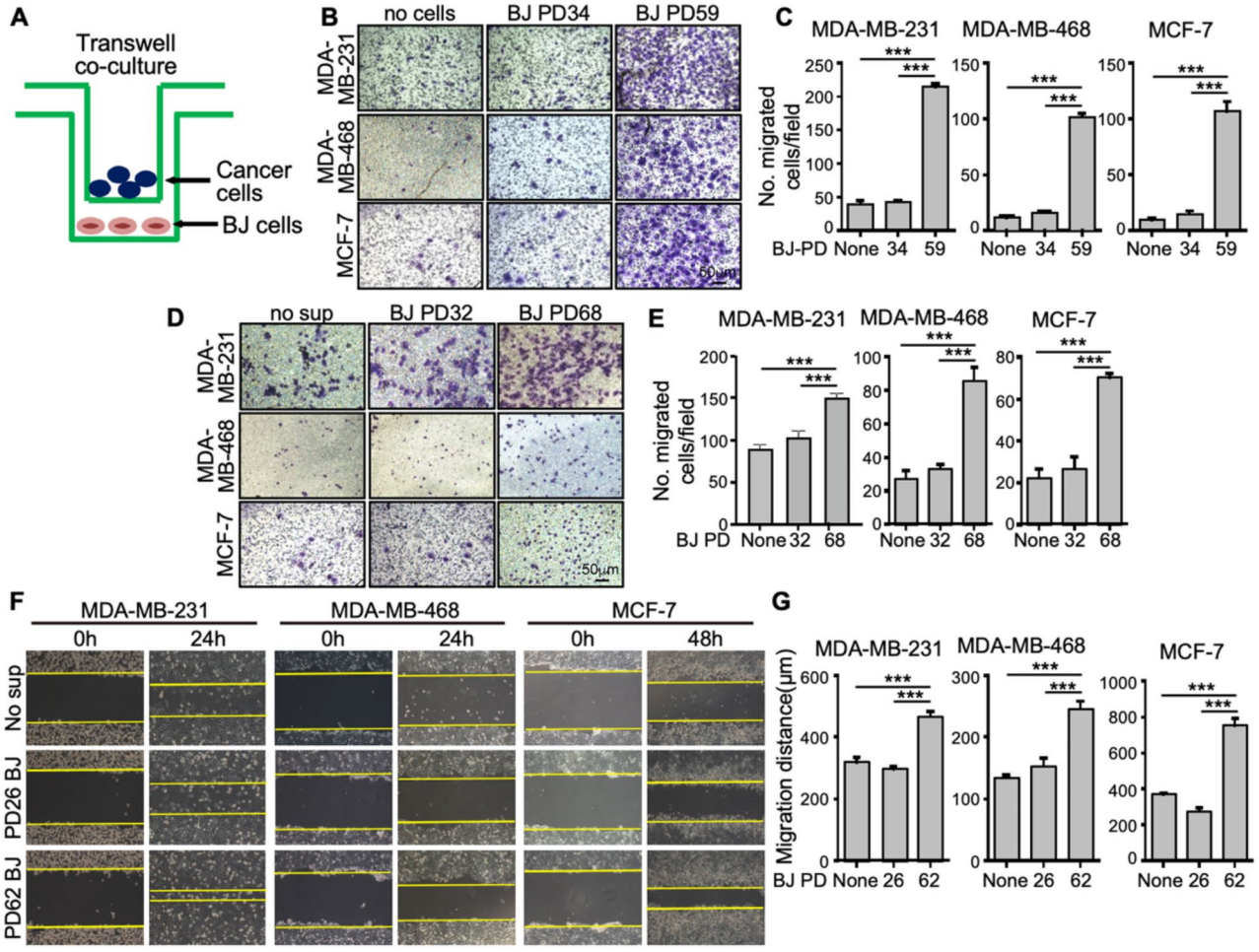

Fig. 1 Senescent BJ cells promote the motility of breast cancer cells

(**A**) Schematic diagram of the co-culture system in which young or senescent BJ cells and breast cancer cells were seeded in the lower and upper chambers, respectively, of the transwells. The 2 chambers were separated by a membrane with 8-micron pores. Migration of the breast cancer cells towards the lower chamber was measured. (**B**-**C**) Representative crystal violet-stained images of transwell migration of MDA-MB-231, MDA-MB-468 and MCF-7 cells co-cultured with medium (no cells or None) or young (PD34) or senescent (PD59) BJ cells for 12 h (**B**), and quantification of number of migrated cells per 20X field (mean ± SD, $n = 3$) (**C**). At least 5 randomly chosen 20X fields were counted for each of the triplicates. (**D**-**E**) Representative crystal violet-stained images of transwell migration of MDA-MB-231, MDA-MB-468 and MCF-7 cells co-cultured with medium only (no sup or None) or conditioned medium from young (PD32) or senescent (PD68) BJ cells for 16 h (**D**), and quantification of number of migrated cells per 20X field (mean ± SD, $n = 3$) (**E**). At least 5 randomly chosen 20X fields were counted for each of the triplicates. (**F**-**G**) Representative images of MDA-MB-231, MDA-MB-468 and MCF-7 cells immediately (0 h), 24 h (24 h, for MDA-MD-231 and MDA-MB-468) or 48 h (48 h, for MCF-7) after a scratch wound was made and co-cultured with medium only (no sup or None) or conditioned medium from young (PD26) or senescent (PD62) BJ cells (**F**), and quantification of the distance (μM) of the wound edges by ImageJ at 24 h (for MDA-MD-231 and MDA-MB-468) or 48 h (for MCF-7) (mean ± SD, $n = 3$) (**G**). (**C**, **E**, **G**) *** $p < 0.001$ between indicated groups in One-way ANOVA corrected for multiple comparisons using Tukey's multiple comparison correction adjustment

(MDA-MB-231, MDA-MB-468 and MCF-7), co-culture with senescent, but not with young, BJ cells (Fig. S1A), stimulated the migration of the cancer cells through the transwells (Fig. 1B-C). Similarly, incubation with the conditioned medium collected from senescent cells (Fig. S1B) present in the lower chamber promoted the migration of breast cancer cells in transwells, while that collected from young BJ cells failed to do so (Fig. 1D-E). The conditioned medium from senescent BJ cells, but not that from young BJ cells (Fig. S1C), also increased the motility of the breast cancer cells in wound healing assays (Fig. 1F-G).

Epithelial-mesenchymal transition (EMT), characterized by loss of cell-cell junctions, is a key feature of increased motility in cancer cells of epithelial origins [14, 15]. Western blotting analysis revealed that co-culture with senescent BJ cells, but not with young BJ cells (Fig. S1D), in the transwells decreased the expression of an epithelial cell marker E-cadherin and increased the expression of a mesenchymal cell marker vimentin [16, 17] (Fig. S2A). In addition, in immunofluorescence

staining assays, co-culture with senescent cells, but not with young cells, reduced E-cadherin signals in MDA-MB-231, MDA-MB-468 and MCF-7 cells, and also the cell surface localization of E-cadherin in MDA-MB-468 and MCF-7 cells (Fig. S2B). There results indicate that senescent cells promote EMT, consistent with the increased motility, in breast cancer cells.

Taken together, these results indicate that factors secreted by the senescent BJ fibroblasts promote the motility of breast cancer cells.

Senescent BJ cells secrete GM-CSF and bFGF as part of SASP

In order to identify the senescent BJ cell-secreted factors that promote breast cancer cell motility, we searched the literature for SASP factors with known functions in cell movement. Among the SASP factors (GRO-α,-β,-γ, GM-CSF, IL-7, MCP-2, IL-13, ICAM-3, TRAIL-R3, Fas/TNFRSF6, IGFBP-6, and bFGF) secreted by BJ cells induced to undergo senescence by 20% oxygen [18], GM-CSF [19–22], bFGF [23–27] and CXCL1 [28–32] have been reported to promote cell migration.

We thus compared the mRNA levels of GM-CSF, bFGF, and CXCL1 using qRT-PCR and their protein levels in conditioned media using ELISA, in senescent and young BJ cells (Fig. S1D). While the mRNA levels of GM-CSF, bFGF, and CXCL1 were all increased in the senescent BJ cells as compared with young BJ cells (Fig. 2A), only GM-CSF and bFGF proteins, but not that of CXCL1, were present at higher levels in the conditioned medium from senescent BJ cells than the young BJ cells (Fig. 2B). Therefore, we focused on GM-CSF and bFGF, and investigated their roles in the ability of senescent cells to promote breast cancer cell motility.

Senescent cells promote the motility of breast cancer cells through GM-CSF and bFGF

It has been reported that GM-CSF stimulates Lewis lung cancer cell metastasis via protein kinase A (PKA) [33], and promotes the proliferation and invasion of lung cancer cells by activating MEK1/ERK and PI3K/

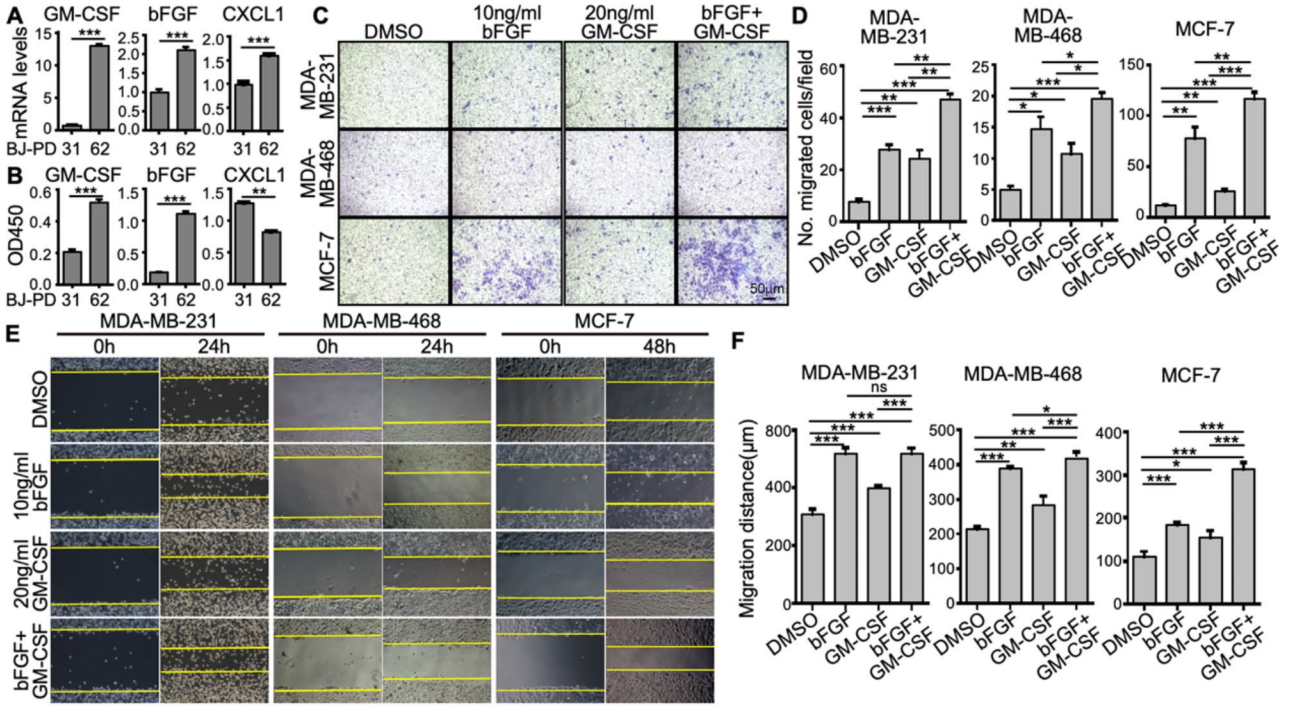

Fig. 2 Senescent cells secrete bFGF and GM-CSF that promote the motility of breast cancer cells

(**A**) Relative mRNA levels (mean ± SD, $n = 3$) of GM-CSF, bFGF and CXCL1 in young (PD31) and senescent (PD62) BJ cells as determined by quantitative real time PCR analysis. (**B**) Relative protein levels (mean ± SD, $n = 3$) of GM-CSF, bFGF and CXCL1 in the conditioned medium from young (PD31) and senescent (PD62) BJ cells as determined by ELISA. (**C**-**D**) Representative crystal violet-stained images of transwell migration of MDA-MB-231, MDA-MB-468 and MCF-7 cells co-cultured with medium containing DMSO, 10 ng/ml of bFGF, 20 ng/ml of GM-CSF or both for 12 h (**C**), and quantification of number of migrated cells per field (mean ± SD, $n = 3$) (**D**). At least 5 randomly chosen 20X fields were counted for each of the triplicates. (**E**-**F**) Representative images of MDA-MB-231, MDA-MB-468 and MCF-7 cells immediately (0 h), 24 h (24 h, for MDA-MB-231 and MDA-MB-468) or 48 h (48 h, for MCF-7) after a scratch wound was made and co-cultured with medium containing DMSO, 10 ng/ml of bFGF, 20 ng/ml of GM-CSF or both (**E**), and quantification of the distance of the wound edges by ImageJ at 24 h (for MDA-MB-231 and MDA-MB-468) or 48 h (for MCF-7) (mean ± SD, $n = 3$) (**F**). (**A**-**B**, **D**, **F**) * $p < 0.05$, ** $p < 0.01$ and *** $p < 0.001$ vs. BJ-PD31 in unpaired, 2-sample t-tests (**A**-**B**) or between indicated groups in One-way ANOVA corrected for multiple comparisons using Tukey's multiple comparison correction adjustment (**D**, **F**)

AKT pathways [21], and that bFGF promotes pancreatic cancer cell invasion in cell culture, and drives cancer cell dissemination in vivo [34]. We thus investigated whether GM-CSF and bFGF secreted by senescent cells can promote the motility of breast cancer cells. Indeed, bFGF and GM-CSF added to the lower chambers of transwells promoted the migration of the MDA-MB-231, MDA-MB-468 and MCF-7 breast cancer cells seeded in the upper chambers, as compared to the vehicle control (DMSO); and combination of bFGF and GM-CSF had a stronger effect than GM-CSF or bFGF alone (Fig. 2C-D). Similar results were obtained in wound healing assays, although the effect of bFGF and GM-CSF combination was not as obvious in MDA-MB-231 and MDA-MB-468 cells as in the transwell assays (Fig. 2E-F). These findings indicate that GM-CSF and bFGF increase the motility of breast cancer cells.

To determine whether the ability of senescent cells to promote breast cancer motility relied on GM-CSF and bFGF, we utilized neutralizing antibodies against these proteins. When senescent cells (Fig. S1E) were incubated with a neutralizing antibody against bFGF or GM-CSF in the lower chamber of the transwells, the migration of the breast cancer cells was greatly reduced as compared to when senescent cells were incubated with an anti-β-actin antibody or when left untreated (Fig. 3A-B). Incubation with both neutralizing antibodies against bFGF or GM-CSF further decreased the ability of senescent cells to induce breast cancer cell migration, in comparison to when only bFGF or GM-CSF alone was depleted (Fig. 3A-B). To further validate the results obtained with neutralizing antibodies, we generated shRNAs that silenced bFGF or GM-CSF expression in young and senescent BJ cells (Fig. S1E, S3A-B), and the most effective shRNAs (bFGF-sh1 and GM-CSF-sh4) were tested further for their effects on cell motility. Silencing of bFGF or GM-CSF in senescent cells abrogated senescent cell-induced breast cancer cell migration in transwells, while silencing of bFGF or GM-CSF in young BJ cells had no effect on breast cancer cell migration (Fig. 3C-D). Thus, bFGF and GM-CSF are the major SASP factors secreted by senescent cells, which are capable of inducing breast cancer cell migration.

Taken together, our results demonstrate that senescent cells secrete bFGF and GM-CSF, which in turn promote breast cancer cell motility.

The JNK pathway mediates senescent cell-induced breast cancer cell migration

We next investigated the signaling pathway in breast cancer cells which mediates senescent cell-induced motility. It has been reported that both bFGF and GM-CSF

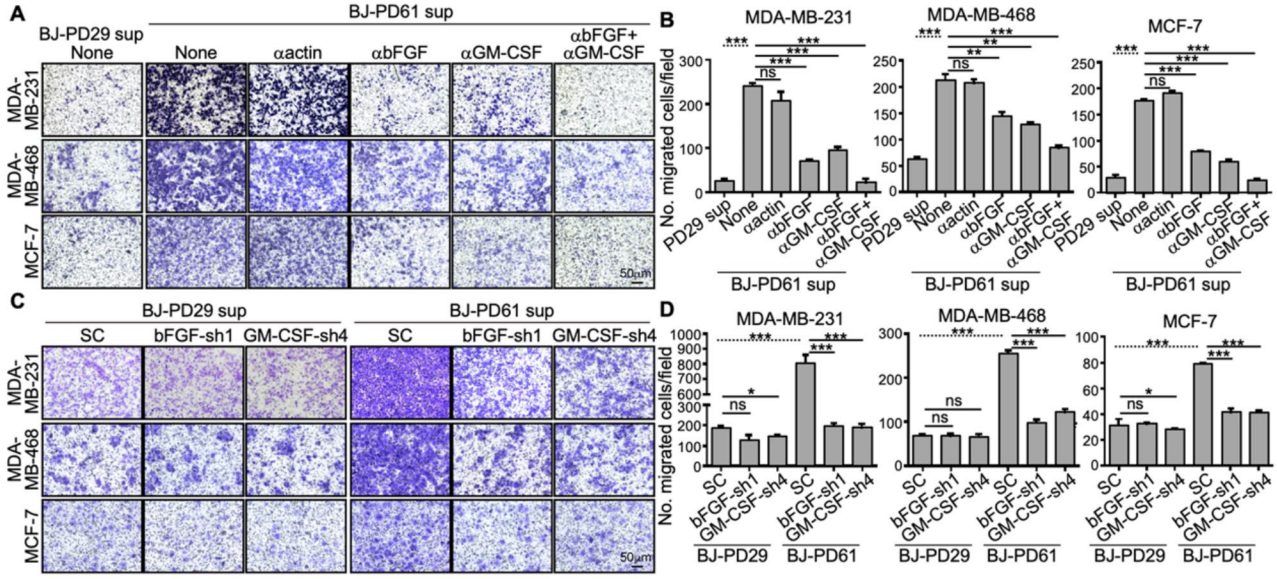

Fig. 3 Senescent cells promote the migration of breast cancer cells via secreted bFGF and GM-CSF. (**A**-**B**) Representative crystal violet-stained images of transwell migration of MDA-MB-231, MDA-MB-468 and MCF-7 cells co-cultured with conditioned medium from young (PD29) or senescent (PD61) BJ cells, which were left untreated (None) or incubated with neutralizing antibodies against β-actin (1 ng/ml), bFGF (1 ng/ml), GM-CSF (5 ng/ml) or both bFGF and GM-CSF for 12 h (**A**), and quantification of number of migrated cells per field (mean ± SD, $n = 3$) (**B**). At least 5 randomly chosen 20X fields were counted for each of the triplicates (**C**-**D**) Representative crystal violet-stained images of transwell migration of MDA-MB-231, MDA-MB-468 and MCF-7 cells co-cultured with conditioned medium from young (PD29) or senescent (PD61) BJ cells transduced with shRNA control (SC) or shRNAs for bFGF or GM-CSF for 20 h (**C**), and quantification of number of migrated cells per field (mean ± SD, $n = 3$) (**D**). At least 5 randomly chosen 20X fields were counted for each of the triplicates. (**B**, **D**) ns, not significant; * $p < 0.05$; ** $p < 0.01$; and *** $p < 0.001$ between indicated groups in unpaired, 2-sample t tests (dotted lines) or One-way ANOVA corrected for multiple comparisons using Tukey's multiple comparison correction adjustment (solid lines)

can induce the signaling of the STAT3, PI3K/AKT, ERK and JNK pathways [19, 21, 35–38]. Western blotting analysis revealed that co-cultured senescent cells, but not the young cells (Fig. S1F), markedly and consistently increased the activating phosphorylation of JNK in all 3 breast cancer cells (Fig. 4A-B), suggesting a universal role of the JNK pathway in senescent cell-induced breast cancer cell migration. Phosphorylation of Stat3, AKT and ERK was induced by senescent cells moderately in some, but not all, of these breast cancer cell lines, and phosphorylation of Stat3 appeared to be increased by both senescent and young BJ cells in MDA-MB-231 and MCF-7 cells (Fig. 4A-B). While activated ERK and other proteins such as AKT may play a role in senescent cell-stimulated migration in some cells, we focused our investigation on JNK, which was activated by senescent BJ cells, but not by young BJ cells, in all 3 breast cancer cells tested in this study.

The induction of JNK phosphorylation in breast cancer cells by senescent BJ cells relied on GM-CSF and bFGF, as neutralization of GM-CSF and/or bFGF abrogated the induction of JNK phosphorylation in MDA-MB-231 and MDZ-MB-468 cells by co-cultured senescent BJ cells (Fig. S1F, 4 C-D). Furthermore, GM-CSF and bFGF, alone or in combination, induced JNK phosphorylation in both MDA-MB-231 and MDA-MB-468 cells (Fig. 4E,

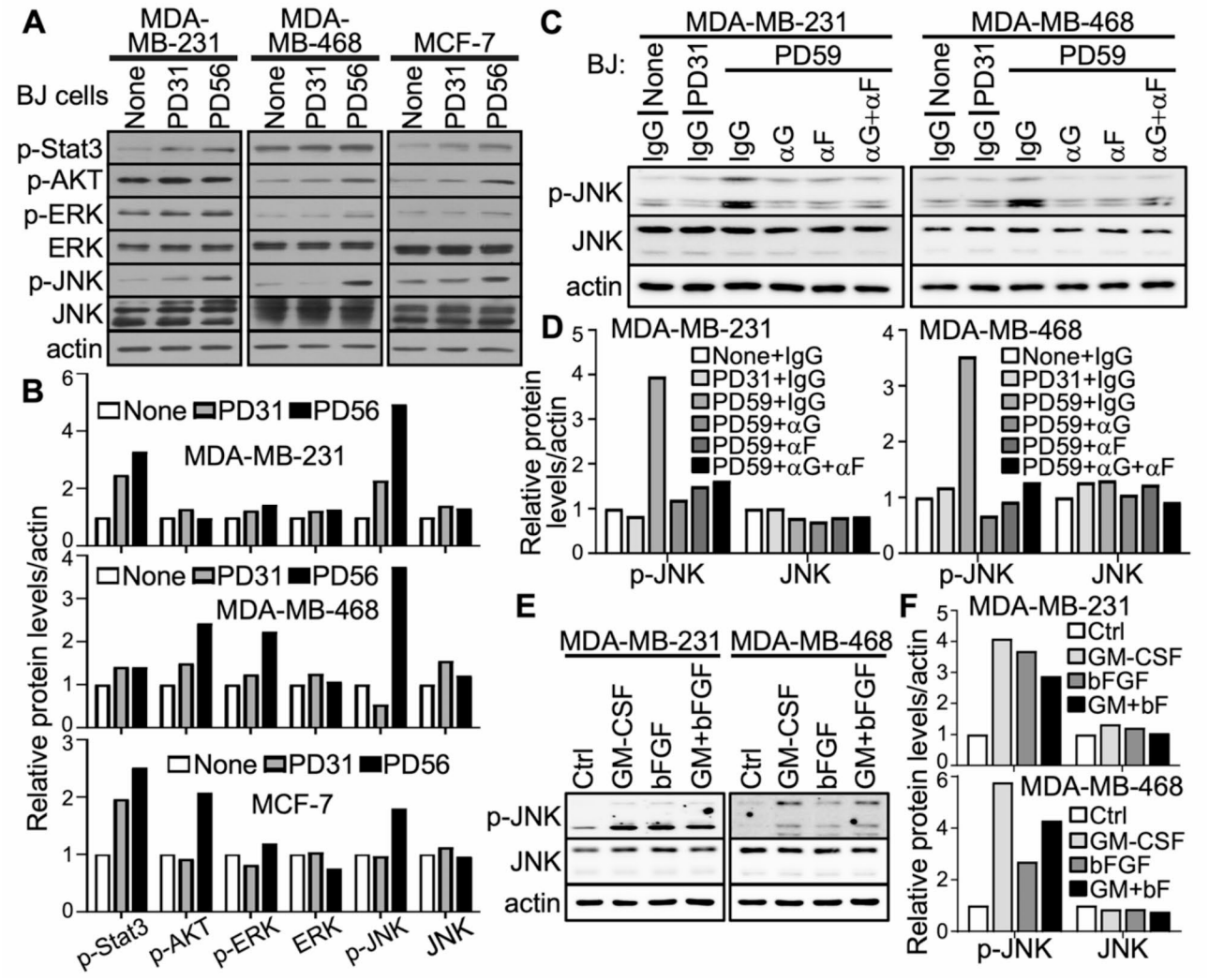

Fig. 4 Senescent cells induce JNK activation via secreted GMCSF and bFGF

(**A**-**B**) Western blotting analysis of the phosphorylation/activation status of Stat3, AKT, ERK and JNK in MDA-MB-231, MDA-MB-468 and MCF-7 breast cancer cell lines co-cultured with medium (None) or young (PD31) or senescent (PD56) BJ cells. (**C**-**D**) Western blotting analysis of phosphorylated/activated JNK in MDA-MB-231 and MDA-MB-468 breast cancer cell lines co-cultured with medium (None) or young (PD31) or senescent (PD59) BJ cells, which were incubated with neutralizing antibodies against IgG, GM-CSF (αG, 5 ng/ml), bFGF (αF, 1 ng/ml), or both bFGF and GM-CSF (αG + αF). (**E**-**F**) Western blotting analysis of phosphorylated/activated JNK in MDA-MB-231 and MDA-MB-468 breast cancer cell lines treated with GM-CSF, bFGF or both. (**B**, **D**, **F**) Quantification of the Western blot results presented in A, C and E, respectively, showing expression levels of indicated proteins relative to None (**B**), None + IgG (**D**) or Ctrl (**F**). Densitometric quantification of bands in the Western blots was performed by ImageJ. The signals were normalized to that of actin

F). Therefore, GM-CSF and bFGF are both necessary and sufficient for the activation of JNK.

We knocked down JNK1 and JNK2 by shRNAs in MDA-MB-231 and MDA-MB-468 breast cancer cells (Fig. 5A). Both JNK1 and JNK2 shRNAs abrogated senescent BJ cell (Fig. S1F)-induced breast cancer cell migration in transwells, but neither JNK1 shRNAs nor JNK2 shRNAs had significant effects in breast cancer cells co-cultured with young BJ cells (Fig. 5B-C). Similarly, JNK1 and JNK2 shRNAs disrupted migration of MDA-MB-231 and MDA-MB-468 cells cultured in the presence of GM-CSF and/or bFGF, but had no effect on breast cancer cells cultured with saline control (Fig. 5D-E, S4).

These results indicate that senescent cell-secreted GM-CSF and bFGF induce breast cancer cell migration by activating the signaling pathway involving both JNK1 and JNK2 in cancer cells.

Senescent fibroblast cells promote breast cancer metastasis in xenograft tumor models

To investigate the effect of senescent cells on breast cancer metastasis in vivo, we co-injected MDA-MB-231 cells with young or senescent BJ cells (Fig. S1G) into the mammary fat pad of nude mice, and monitored primary tumor growth rate, and analyzed lung metastasis at the endpoints. Within the time window of observation (9 weeks), tumors generated from co-injection with

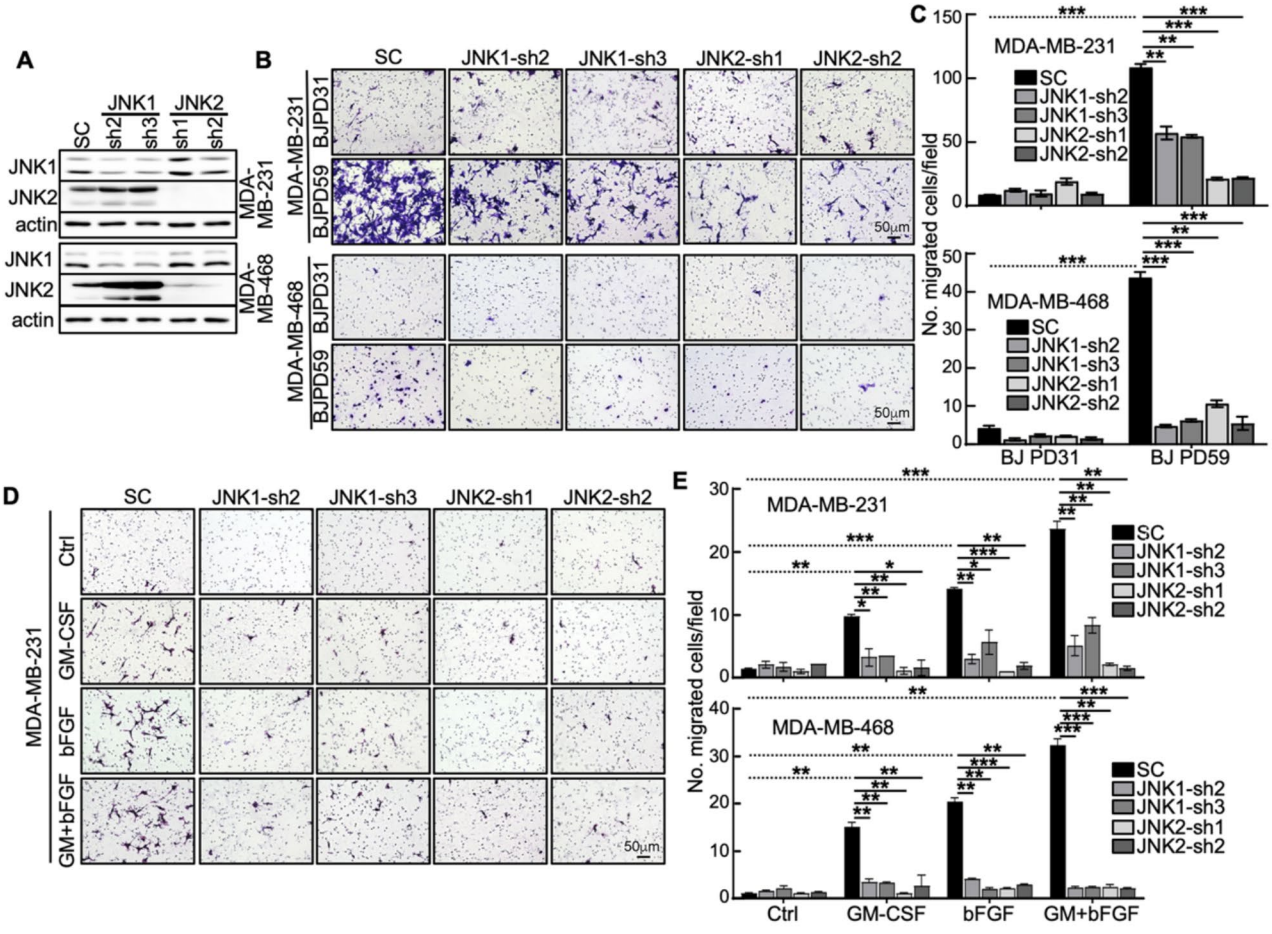

Fig. 5 JNK mediates the stimulation of breast cancer migration by senescent cell-secreted GM-CSF and bFGF

(**A**) Western blotting analysis showing knockdown specificity and efficiency of JNK1 and JNK2 shRNAs in MDA-MB-231 and MDA-MB-468 cells. (**B**-**C**) Representative crystal violet-stained images of transwell migration of MDA-MB-231 and MDA-MB-468 cells co-cultured with young (PD31) or senescent (PD59) BJ cells transduced with shRNA control (SC) or shRNAs for JNK1 or JNK2 for 12 h (**C**), and quantification of number of migrated cells per field (mean ± SD, $n = 3$) (**D**). At least 5 randomly chosen 20X fields were counted for each of the triplicates. (**D**-**E**) Representative crystal violet-stained images of transwell migration of MDA-MB-231 cells transduced with shRNAs for JNK1 or JNK2 or shRNA control (SC) and treated with vehicle control, 20 ng/ml of GM-CSF, 10 ng/ml of bFGF or both for 12 h (**D**), and quantification of number per field (mean ± SD, $n = 3$) of migrated MDA-MB-231 and MDA-MB-468 cells transduced with shRNAs for JNK1 or JNK2 or shRNA control (SC) and treated with vehicle control, 20 ng/ml of GM-CSF, 10 ng/ml of bFGF or both for 13 h (**E**). At least 5 randomly chosen 20X fields were counted for each of the triplicates. (**C**, **E**) $^{**}p < 0.01$ and $^{***}p < 0.001$ between indicated groups in unpaired, 2-sample t tests (dotted lines) or One-way ANOVA corrected for multiple comparisons using Tukey's multiple comparison correction adjustment (solid lines)

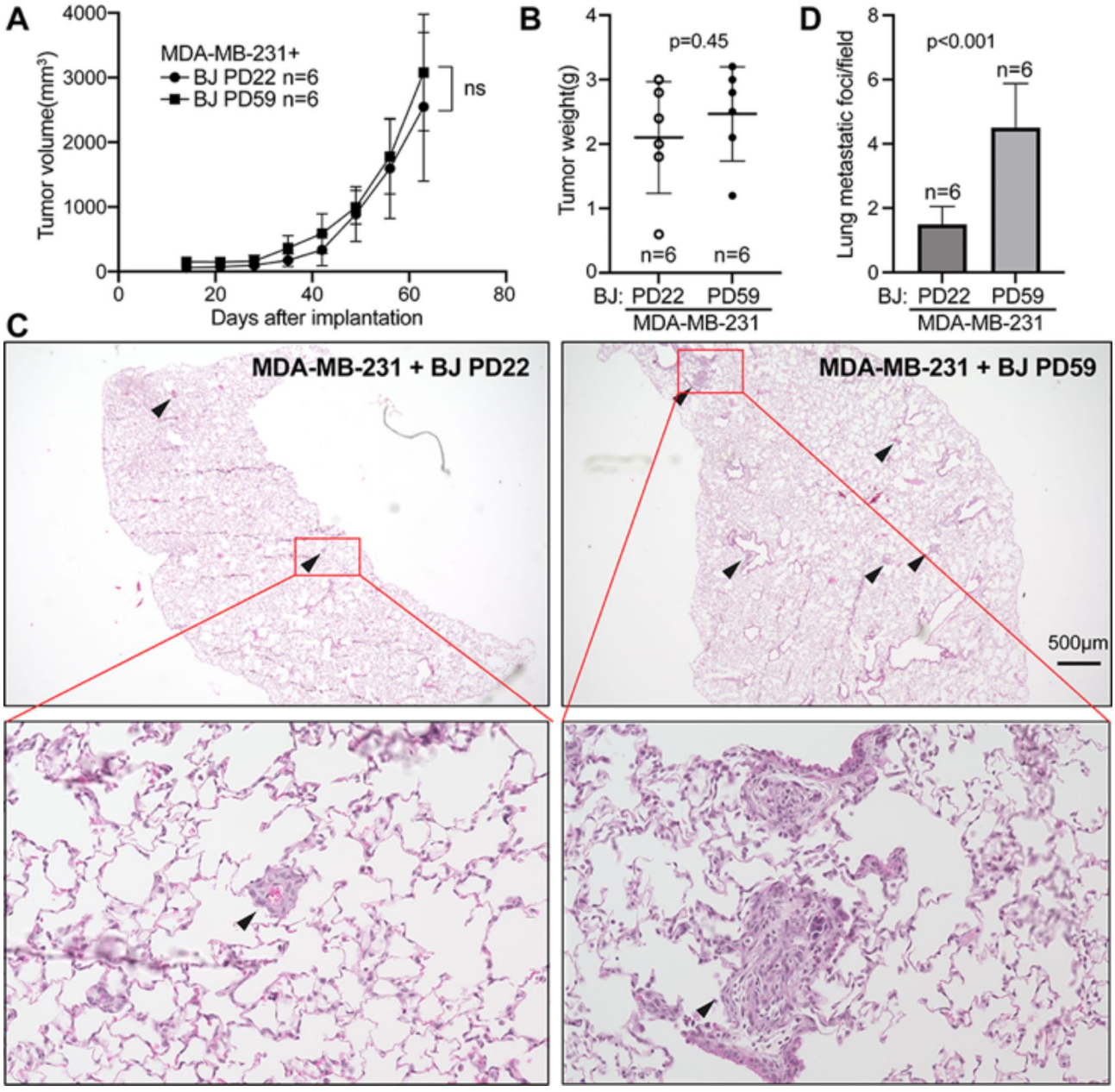

Fig. 6 Senescent cells promote breast cancer metastasis in xenograft tumor models. 5×10^5 of MDA-MB-231 cells and 5×10^5 of young (PD22) or senescent (PD59) BJ cells were co-injected into the mammary fat pads of 6–8-week-old nude mice. Tumor sizes were measured weekly over 9 weeks. Tumor growth curves were plotted (**A**). Upon sacrifice, tumors were removed and weighted (**B**), and lung sections were stained by hematoxylin and eosin, photographed (**C**) and quantified for the number of metastatic foci (indicated by arrows) (**D**). In (**C**), images of the representative lung sections with metastatic foci (indicated by arrows) are shown in the top panels, and one metastatic focus (indicated by red boxes) from each section is magnified and shown in the bottom panels. In (**D**), for each mouse among the total of 6 in each group, the number of metastatic foci were counted in 5 randomly chosen 2X fields in a section containing all 5 lung lubes, and the number of metastatic foci per field was calculated. (**A**-**B**, **D**) Values are mean ± SD, $n = 6$ mice per group. p values are from unpaired, 2-sample t tests. ns, not significant

senescent BJ cells and those with young cells showed no significant difference in grow rate (Fig. 6A), or in weight or size at the time of sacrifice (Fig. 6B, S5). However, co-injected senescent cells greatly enhanced lung metastasis as compared to the young cells (Fig. 6C-D). Therefore, at least under the experimental conditions used in the current study, senescent cells specifically promote breast cancer cell metastasis in vivo, without significant effects on the growth of the primary tumors.

Discussion

Cellular senescence has been recognized as a double-edged sword in cancer development [7]. While the intracellular activation of senescence programs serves as a tumor suppressing mechanisms by limiting the growth of cells with oncogenic potential and genome instability and enhancing the sensitivity to cancer therapies, it promotes cancer development in a paracrine fashion via SASP factors [39]. The current study demonstrates that senescent cells promote the motility and metastasis of breast cancer cells. Although older age correlates with high incidence, poor prognosis and metastasis in many cancer types [40, 41], the relationship among patient age, metastasis and prognosis is complex in breast cancer. While older women (>60y) have poorer prognosis at the metastatic stage, young age is associated with an aggressive presentation but has no impact on overall survival in metastatic breast cancer [42]. This is likely due to the presence of multifactorial modulators of the disease, including levels of various hormones, besides aging. Nevertheless, while senescent cells increase with age in human tissues [43–45], which can certainly impact cancer progression, cellular senescence can also be induced by other stimuli, such as oncogene activation and loss of tumor suppressor genes, and several types of stresses, including oxidative stress and stresses caused by chemotherapy, irradiation, cytokine treatment, and induced pluripotent stem (iPS) cell reprogramming [46, 47]. Despite the causes, these different types of senescence can all contribute to metastasis and other aspects of tumor development via the SASP factors in breast cancer. Furthermore, in addition to breast cancer, our findings can be applied to other cancer types, including those in which organism aging and other senescence inducers are risk factors for metastasis.

We found that senescent fibroblasts secret GM-CSF and bFGF, which activates JNK1 and JNK2 in breast cancer cells, leading to increased motility of the cancer cells. An earlier study by Coppe et al. indicated that conditioned medium from senescent cells stimulated the ability of breast cancer cells to invade a basement membrane via IL-6 and IL-8 [18]. However, the effect of senescent cells on cancer cell motility was unclear. Our study has thus identified GM-CSF and bFGF as the SASP factors that mediate the induction of cancer cell motility by senescent fibroblasts. We were unable to detect an increase in IL-6 and IL-8 levels in senescent BJ cells when they were cultured in 20% oxygen incubators (data not shown). Indeed, in the Coppe study, the expression of IL-6 and IL-8 was significantly increased in senescent BJ cells maintained in 3%, but not 20%, oxygen [18]. Nevertheless, the contribution of other SASP factors, including IL-6 and IL-8, in the tumor microenvironment, to cancer cell motility cannot be excluded. It is highly likely that senescent stromal cells promote cancer cell migration, and ultimately metastasis, through the corporative action of multiple SASP factors in a context-dependent fashion.

We further demonstrated that senescent fibroblasts stimulated the lung metastasis of xenograft tumors when co-injected with MDA-MB-231 cells, as compared to the young, pre-senescent fibroblasts. In addition to GM-CSF and bFGF that enhance cancer cell motility as demonstrated in this study, various SASP factors have been reported to promote other metastasis-related phenotypes in a context dependent manner, including invasion, Epithelial-mesenchymal transition (EMT), extracellular matrix degradation, and tumor vascularization [7]. It is likely that at least some of these other SASP factors may also contribute to the metastasis-promoting effect of the senescent cells we observed in the orthotopic xenograft models.

In our study, senescent BJ cells promoted lung metastasis without significantly altering the growth rate of primary tumors in the xenograft models. This was in contrast with a previous report indicating that co-injection of MDA-MB-231 cells with senescent fibroblasts (WI-38) at a 1:4 ratio promoted both tumor incidence and tumor growth rate, as compared to that with pre-senescent fibroblasts or MDA-MB-231 cells alone, in a xenograft tumor model [5], suggesting that senescent fibroblasts facilitate tumor growth. Since the current study focused on the role of senescent cells in cancer metastasis, in order to minimize the contribution of primary tumor size to metastasis, we chose to sacrifice the mice and examine lung metastasis when the size of the primary tumors did not differ significantly. Indeed, at later time points, tumors from the group co-injected with senescent cells were larger than those from co-injection with young BJ cells. Other differences in the experimental settings may also contribute to the differential effects of senescent cells on primary tumor growth. We co-injected cancer cells with BJ cells, whose SASP program may differ from that of WI-38 cells used in the prior report [5]. In addition, the ratio of injected senescent fibroblasts and cancer cells was 1:1 in our study, and was 4 times lower than what was used in the previous study (4:1) [5], which may alter the relative effects of senescent cells on tumor growth and metastasis.

Conclusions

We have identified a novel mechanism by which senescent cells promote cancer metastasis and progression. Senescent cells increase the motility of breast cancer cells through secretion of GM-CSF and bFGF, which in turn induces activation of the JNK pathway in cancer cells. More importantly, senescent cells promoted breast cancer metastasis, with a minimum effect of the primary tumor growth, in orthotopic xenograft mouse models. These results will potentially lead to identification of novel targets for cancer therapies that suppress metastasis, the major cause of cancer mortality.

Supplementary Information

The online version contains supplementary material available at https://doi.org/10.1186/s12964-024-01861-x.

Supplementary Material 1

Acknowledgements
We thank Cell Engineering Shared Resource, and Tumor Tissue and Pathology Shared Resource of AHWFBCCC for support (P30CA012197).

Author contributions
NW, YL, SY, HL, RX and PS conceived and designed the study. NW, YH, YF, SH, DC, and HW executed the experiments; NW, YH, YF, SH, DC, HW, RX and PS analyzed and interpreted the data, EVD guided the statistical analyses; NW and PS wrote and edited the manuscript.

Funding
This study was supported by NIH/NCI grants (CA131231 and CA172115) (PS), and the China Scholarship Council (NW, YH). PS is an Anderson Oncology Research Professor.

Data availability
No datasets were generated or analysed during the current study.

Declarations

Ethics approval and consent to participate
All the animal studies were approved by in the Institutional Animal Care and Use Committee (IACUC) at Wake Forest University School of Medicine.

Consent for publication
N/A.

Competing interests
The authors declare no competing interests.

Author details
[1]The Second Surgical Department of Breast Cancer, Tianjin Medical University Cancer Institute & Hospital, Key Laboratory of Cancer Prevention and Therapy, National Clinical Research Center for Cancer, Tianjin, China
[2]School of Medicine, Nankai University, Tianjin, China
[3]Department of Cancer Biology, Wake Forest University School of Medicine, Atrium Health Wake Forest Baptist Comprehensive Cancer Center, Winston-Salem, NC, USA
[4]Department of Biostatistics and Data Science, Wake Forest University School of Medicine, Atrium Health Wake Forest Baptist Comprehensive Cancer Center, Winston-Salem, NC, USA
[5]Department of General Surgery, Jiangnan University Medical Center, Wuxi, China
[6]Department of Pharmacy, Nanfang Hospital, Southern Medical University, Guangzhou, Guangdong, China
[7]Department of Medicine, Memorial Sloan Kettering Cancer Center, New York, NY, USA
[8]College of Life Sciences, Hebei Agricultural University, Baoding, China
[9]Breast Cancer Center, Chongqing University Cancer Hospital, Chongqing, China

Received: 9 June 2024 / Accepted: 30 September 2024
Published online: 07 October 2024

References

1. Parkin DM. Global cancer statistics in the year 2000. Lancet Oncol. 2001;2(9):533–43.
2. Coppe JP, Kauser K, Campisi J, Beausejour CM. Secretion of vascular endothelial growth factor by primary human fibroblasts at senescence. J Biol Chem. 2006;281(40):29568–74.
3. Laberge RM, Awad P, Campisi J, Desprez PY. Epithelial-mesenchymal transition induced by senescent fibroblasts. Cancer Microenvironment: Official J Int Cancer Microenvironment Soc. 2012;5(1):39–44.
4. Campisi J. Cancer, aging and cellular senescence. vivo. 2000;14(1):183–8.
5. Krtolica A, Parrinello S, Lockett S, Desprez PY, Campisi J. Senescent fibroblasts promote epithelial cell growth and tumorigenesis: a link between cancer and aging. Proc Natl Acad Sci USA. 2001;98(21):12072–7.
6. Lecot P, Alimirah F, Desprez PY, Campisi J, Wiley C. Context-dependent effects of cellular senescence in cancer development. Br J Cancer. 2016;114(11):1180–4.
7. Xiao S, Qin D, Hou X, Tian L, Yu Y, Zhang R, et al. Cellular senescence: a double-edged sword in cancer therapy. Front Oncol. 2023;13:1189015.
8. Elkhattouti A, Hassan M, Gomez CR. Stromal fibroblast in Age-Related Cancer: role in Tumorigenesis and potential as Novel Therapeutic Target. Front Oncol. 2015;5:158.
9. Kim E, Rebecca V, Fedorenko IV, Messina JL, Mathew R, Maria-Engler SS, et al. Senescent fibroblasts in melanoma initiation and progression: an integrated theoretical, experimental, and clinical approach. Cancer Res. 2013;73(23):6874–85.
10. Bhowmick NA, Neilson EG, Moses HL. Stromal fibroblasts in cancer initiation and progression. Nature. 2004;432(7015):332–7.
11. Malaquin N, Vercamer C, Bouali F, Martien S, Deruy E, Wernert N, et al. Senescent fibroblasts enhance early skin carcinogenic events via a paracrine MMP-PAR-1 axis. PLoS ONE. 2013;8(5):e63607.
12. Fang Y, Wang J, Wang G, Zhou C, Wang P, Zhao S, et al. Inactivation of p38 MAPK contributes to stem cell-like properties of non-small cell lung cancer. Oncotarget. 2017;8(16):26702–17.
13. Chang A, Chen Y, Shen W, Gao R, Zhou W, Yang S, et al. Ifit1 protects against Lipopolysaccharide and D-galactosamine-Induced Fatal Hepatitis by inhibiting activation of the JNK pathway. J Infect Dis. 2015;212(9):1509–20.
14. Thiery JP, Acloque H, Huang RY, Nieto MA. Epithelial-mesenchymal transitions in development and disease. Cell. 2009;139(5):871–90.
15. Vleminckx K, Vakaet L Jr., Mareel M, Fiers W, van Roy F. Genetic manipulation of E-cadherin expression by epithelial tumor cells reveals an invasion suppressor role. Cell. 1991;66(1):107–19.
16. Peinado H, Portillo F, Cano A. Transcriptional regulation of cadherins during development and carcinogenesis. Int J Dev Biol. 2004;48(5–6):365–75.
17. Kokkinos MI, Wafai R, Wong MK, Newgreen DF, Thompson EW, Waltham M. Vimentin and epithelial-mesenchymal transition in human breast cancer–observations in vitro and in vivo. Cells Tissues Organs. 2007;185(1–3):191–203.
18. Coppe JP, Patil CK, Rodier F, Sun Y, Munoz DP, Goldstein J, et al. Senescence-associated secretory phenotypes reveal cell-nonautonomous functions of oncogenic RAS and the p53 tumor suppressor. PLoS Biol. 2008;6(12):2853–68.
19. Aliper AM, Frieden-Korovkina VP, Buzdin A, Roumiantsev SA, Zhavoronkov A. A role for G-CSF and GM-CSF in nonmyeloid cancers. Cancer Med. 2014;3(4):737–46.
20. Pyonteck SM, Akkari L, Schuhmacher AJ, Bowman RL, Sevenich L, Quail DF, et al. CSF-1R inhibition alters macrophage polarization and blocks glioma progression. Nat Med. 2013;19(10):1264–72.
21. Uemura Y, Kobayashi M, Nakata H, Kubota T, Bandobashi K, Saito T, et al. Effects of GM-CSF and M-CSF on tumor progression of lung cancer: roles of MEK1/ERK and AKT/PKB pathways. Int J Mol Med. 2006;18(2):365–73.
22. Park BK, Zhang H, Zeng Q, Dai J, Keller ET, Giordano T, et al. NF-kappaB in breast cancer cells promotes osteolytic bone metastasis by inducing osteoclastogenesis via GM-CSF. Nat Med. 2007;13(1):62–9.

23. Kamura S, Matsumoto Y, Fukushi JI, Fujiwara T, Iida K, Okada Y, et al. Basic fibroblast growth factor in the bone microenvironment enhances cell motility and invasion of Ewing's sarcoma family of tumours by activating the FGFR1-PI3K-Rac1 pathway. Br J Cancer. 2010;103(3):370–81.
24. Chen JL, Fan J, Chen MX, Dong Y, Gu JZ. Effect of non-anticoagulant N-desulfated heparin on basic fibroblast growth factor expression, angiogenesis, and metastasis of gastric carcinoma in vitro and in vivo. Gastroenterol Res Pract. 2012;2012:752940.
25. Sun XH, Geng XL, Zhang J, Zhang C. miRNA-646 suppresses osteosarcoma cell metastasis by downregulating fibroblast growth factor 2 (FGF2). Tumour Biology: J Int Soc Oncodevelopmental Biology Med. 2015;36(3):2127–34.
26. Zhao H, Liu H, Chen Y, Xin X, Li J, Hou Y, et al. Oligomannurarate sulfate, a novel heparanase inhibitor simultaneously targeting basic fibroblast growth factor, combats tumor angiogenesis and metastasis. Cancer Res. 2006;66(17):8779–87.
27. Erdem H, Yildirim U, Uzunlar AK, Cam K, Tekin A, Kayikci MA, et al. Relationship among expression of basic-fibroblast growth factor, MTDH/astrocyte elevated gene-1, adenomatous polyposis coli, matrix metalloproteinase 9,and COX-2 markers with prognostic factors in prostate carcinomas. Niger J Clin Pract. 2013;16(4):418–23.
28. Acharyya S, Oskarsson T, Vanharanta S, Malladi S, Kim J, Morris PG, et al. A CXCL1 paracrine network links cancer chemoresistance and metastasis. Cell. 2012;150(1):165–78.
29. Tsuyada A, Chow A, Wu J, Somlo G, Chu P, Loera S, et al. CCL2 mediates cross-talk between cancer cells and stromal fibroblasts that regulates breast cancer stem cells. Cancer Res. 2012;72(11):2768–79.
30. Bandapalli OR, Ehrmann F, Ehemann V, Gaida M, Macher-Goeppinger S, Wente M, et al. Down-regulation of CXCL1 inhibits tumor growth in colorectal liver metastasis. Cytokine. 2012;57(1):46–53.
31. Xu J, Zhang C, He Y, Wu H, Wang Z, Song W, et al. Lymphatic endothelial cell-secreted CXCL1 stimulates lymphangiogenesis and metastasis of gastric cancer. Int J Cancer. 2012;130(4):787–97.
32. Kogan-Sakin I, Cohen M, Paland N, Madar S, Solomon H, Molchadsky A, et al. Prostate stromal cells produce CXCL-1, CXCL-2, CXCL-3 and IL-8 in response to epithelia-secreted IL-1. Carcinogenesis. 2009;30(4):698–705.
33. Young MR, Lozano Y, Djordjevic A, Devata S, Matthews J, Young ME, et al. Granulocyte-macrophage colony-stimulating factor stimulates the metastatic properties of Lewis lung carcinoma cells through a protein kinase a signal-transduction pathway. Int J Cancer. 1993;53(4):667–71.
34. Ohuchida K, Mizumoto K, Murakami M, Qian LW, Sato N, Nagai E, et al. Radiation to stromal fibroblasts increases invasiveness of pancreatic cancer cells through tumor-stromal interactions. Cancer Res. 2004;64(9):3215–22.
35. Helsten T, Schwaederle M, Kurzrock R. Fibroblast growth factor receptor signaling in hereditary and neoplastic disease: biologic and clinical implications. Cancer Metastasis Rev. 2015;34(3):479–96.
36. Qian X, Anzovino A, Kim S, Suyama K, Yao J, Hulit J, et al. N-cadherin/FGFR promotes metastasis through epithelial-to-mesenchymal transition and stem/progenitor cell-like properties. Oncogene. 2014;33(26):3411–21.
37. Jaye M, Schlessinger J, Dionne CA. Fibroblast growth factor receptor tyrosine kinases: molecular analysis and signal transduction. Biochim Biophys Acta. 1992;1135(2):185–99.
38. Wang X, Cao X. Regulation of metastasis of pediatric multiple myeloma by MMP13. Tumour Biology: J Int Soc Oncodevelopmental Biology Med. 2014;35(9):8715–20.
39. Birch J, Gil J. Senescence and the SASP: many therapeutic avenues. Genes Dev. 2020;34(23–24):1565–76.
40. Newell GR, Spitz MR, Sider JG. Cancer and age. Semin Oncol. 1989;16(1):3–9.
41. Fane M, Weeraratna AT. How the ageing microenvironment influences tumour progression. Nat Rev Cancer. 2020;20(2):89–106.
42. Frank S, Carton M, Dubot C, Campone M, Pistilli B, Dalenc F, et al. Impact of age at diagnosis of metastatic breast cancer on overall survival in the real-life ESME metastatic breast cancer cohort. Breast. 2020;52:50–7.
43. Dimri GP, Lee X, Basile G, Acosta M, Scott G, Roskelley C, et al. A biomarker that identifies senescent human cells in culture and in aging skin in vivo. Proc Natl Acad Sci U S A. 1995;92(20):9363–7.
44. Wang C, Jurk D, Maddick M, Nelson G, Martin-Ruiz C, von Zglinicki T. DNA damage response and cellular senescence in tissues of aging mice. Aging Cell. 2009;8(3):311–23.
45. Baker DJ, Childs BG, Durik M, Wijers ME, Sieben CJ, Zhong J, et al. Naturally occurring p16(Ink4a)-positive cells shorten healthy lifespan. Nature. 2016;530(7589):184–9.
46. Han J, Sun P. The pathways to tumor suppression via route p38. Trends Biochem Sci. 2007;32(8):364–71.
47. Calcinotto A, Kohli J, Zagato E, Pellegrini L, Demaria M, Alimonti A. Cellular Senescence: aging, Cancer, and Injury. Physiol Rev. 2019;99(2):1047–78.

Publisher's note